

Surface lattice dynamics of Cu(111)

Burl M. Hall and D. L. Mills

*The Institute for Surface and Interface Science and Department of Physics,
University of California, Irvine, California 92717*

Mohamed H. Mohamed and L. L. Kesmodel

Department of Physics, Indiana University, Bloomington, Indiana

(Received 29 March 1988)

We present and analyze off-specular electron-energy-loss data which explore surface vibrations of Cu(111), along the line from $\bar{\Gamma}$ to \bar{M} in the two-dimensional surface Brillouin zone. The dispersion relation of the Rayleigh surface phonon and the longitudinal resonance found in inelastic-He-scattering studies have been measured out to \bar{M} , thus extending the earlier He work. In addition, we obtain the frequency of a (high-frequency) surface phonon which exists at and near \bar{M} , in a gap in the projected bulk-phonon density of states. The data are analyzed within a simple model of surface lattice dynamics. We have also carried out extensive calculations of the energy variation of the various features observed in the electron-loss spectrum, using multiple-scattering theory. Very good agreement between theory and experiment is obtained within a model where the intraplanar force constant between surface atoms is softened by a modest amount, 15%. In our view, the results presented here raise questions about recent suggestions that a very large (70%) softening of the intraplanar surface force constant is present in the Cu(111) surface.

I. INTRODUCTION

The field of surface lattice dynamics has evolved rapidly during recent years. We now have in hand two complementary experimental methods of measuring the dispersion relations of surface phonons and surface resonances, throughout much or perhaps all of the two-dimensional Brillouin zone of both clean and adsorbate covered surfaces. For the first time, theorists have quantitative data alongside which predictions of various models may be placed. The new era was initiated by the appearance of the inelastic-He-scattering studies of LiF by Toennies and his collaborators.¹ Since then, this method has also been applied to the study of the surface vibrations of the surfaces of other alkali halides, semiconductors, and metals. Shortly after the initial He studies appeared, Ibach and co-workers² employed off-specular electron-energy-loss spectroscopy to measure the dispersion relation of the Rayleigh surface phonon on Ni(100). Essential to the success of this and subsequent studies of clean and adsorbate-covered surfaces by inelastic electron scattering is the use of high impact energies (100–300 eV), while resolution sufficient to resolve surface-phonon losses is retained. We now have data in hand on a considerable number of surfaces.

If one surveys the data and analyses on low-index surfaces of metals which also do not reconstruct, one sees that there is clear evidence that surface force constants may differ from those appropriate to the description of the lattice dynamics of the bulk crystal, results that are surely not surprising. The new data, when compared with model calculations, allow one to quantify these changes. On the whole, it is the case that these force-constant changes are rather modest, in the range of

10–20%. Even on surfaces with large surface relaxations, such as those present on Ni(110) (9% contraction between first and second layers), the changes in surface force constants are less than 30%, consistent in magnitude with bond-length-induced changes in force constants encountered in molecular physics.³

A possible exception to these last remarks may be the (111) surfaces of Cu, Ag and Au. Studies of their surface vibrations by the He technique show that in addition to the Rayleigh surface phonon, a prominent resonance with substantial intensity exists within the bulk-phonon bands, quite close to the bottom.⁴ Subsequent theoretical analysis led to the proposal that the resonance was longitudinal in character;⁵ the surface-atom motions are both nearly parallel to the surface and to the wave vector Q_{\parallel} of the resonance. The original analysis, confined to Ag and Au, argued that very large reductions in intraplanar force constants within the surface are essential to explain the data. The reduction required was 50% in Ag and 70% in Au. A recent study concludes that for Cu(111) a 70% reduction is required.⁶

These conclusions are unexpected in our view, particularly for Cu and Ag. There is virtually no surface relaxation in either material, and we know of no data which suggests the presence of the rather substantial changes in electron charge distribution which could produce such very large force-constant modifications in the absence of bond-length changes in the surface region.

We have undertaken new experimental studies of surface vibrations on Cu(111) by off-specular electron-energy-loss spectroscopy and associated theoretical studies, for the following reasons. There is a gap in the projected bulk-phonon density of states at \bar{M} in the surface Brillouin zone, and theories of surface lattice dynamics

predict that a surface phonon exists within this gap.^{7,8} This mode involves primarily longitudinal motion in the surface layer, and since it is quite localized to the surface its frequency is very sensitive to the intraplanar surface force constant, as we shall see. A complete model of the lattice dynamics of this surface must account for not only the longitudinal resonance, but also the frequency of the gap mode, both of which are sensitive to this force constant. The gap mode was not observed in the earlier He work, most likely because its frequency is too high for the mode to be accessed with the beam energies used. Such high-frequency gap modes are readily observed by electron-energy-loss spectroscopy, as earlier work has shown.^{3,9,10} Furthermore, the He data on both the Rayleigh wave and the surface resonance only cover the range from $\bar{\Gamma}$ to roughly two-thirds of the way to \bar{M} . Electron-excitation cross sections do not drop off rapidly with increasing wave-vector transfer as do He-excitation cross sections on smooth metal surfaces, so the zone-boundary region can be accessed with little difficulty. Of course, the energy resolution of the He method is superior, in regions of frequency and wave-vector transfer where vibrational modes are conveniently studied by the method.

We have observed the gap mode at and near \bar{M} , along with the longitudinal resonance and the Rayleigh wave along the entire $\bar{\Gamma}-\bar{M}$ line in the surface Brillouin zone. Our data agree very well with the earlier He work, in the portion of the Brillouin zone where the two data sets overlap. The theoretical analysis consists of two parts. First, we analyze the dispersion relations of the modes within a model of surface lattice dynamics which is quite simple, but which provides a good account of the data. Secondly, for a wide range of energies and two scattering geometries discussed below, we use a multiple-scattering formalism developed¹¹ and employed earlier^{3,9,10} to calculate the electron-energy-loss cross sections. We obtain an excellent, fully quantitative account of the data. It has been established in previous papers^{3,9-11} that the relative intensities of various structures in the loss cross section vary strongly with energy. The theory then confirms our assignment of the various structures observed, and serves as a check on the quality of the eigenvectors and frequencies generated by the lattice-dynamical model. During the course of the research, the theory also guided the choice of beam energies employed, to maximize the cross section of modes of interest.

The physical picture of the lattice dynamics of Cu(111) which emerges from the present study differs qualitatively from that advanced earlier for Ag(111) and Au(111),⁵ and more recently for Cu(111).⁶ We obtain a fully quantitative account of all the data, including the longitudinal resonance and its contribution to the electron-energy-loss cross section, within the framework of a model which invokes a very modest (15%) softening of the intraplanar force constant within the surface. The frequency of the gap mode at \bar{M} , 210 cm^{-1} , lies just a bit below the value we calculate with no change in intraplanar force constant, and very far above that (185 cm^{-1}) we calculate with even a 50% reduction. We also cannot fit the data on the excitation cross section with a reduction as large

as 50%.

Our conclusion is then that the surface force constants which enter the description of the lattice dynamics of Cu(111) differ only modestly from their bulk values, as is the case for a number of other low-index unreconstructed metal surfaces. While we choose a simple model of the bulk and surface lattice dynamics of Cu, we believe it quite adequate for our purpose, and surely capable of discriminating between the physical picture we invoke here, and the dramatic (70%) force-constant reductions proposed elsewhere.⁶

A brief account of our work has appeared elsewhere.¹² This paper presents a full account of our analysis.

The outline of this paper is as follows. Section II is devoted to a discussion of our choice of lattice-dynamical model. Section III discusses the multiple-scattering calculations, and a comparison between these results and the experimental data. Section IV presents our final results and conclusions.

II. BULK PHONONS AND SURFACE VIBRATIONS

We base our analysis on a very simple model phonon spectrum, that generated by the nearest-neighbor central-force model. This contains only one parameter, the second derivative ϕ'' of the nearest-neighbor pair potential. We choose this parameter by minimizing the root-mean-square (rms) deviation between the frequencies generated by the model and the experimental neutron-scattering data.¹³ We have used a value of $2.70 \times 10^4 \text{ dyn/cm}$ for ϕ'' . A comparison between the model and the data is given in Fig. 1; the agreement is very good in our view, and the simple model will prove quite adequate for our purpose. Indeed, it is not clear to us how to improve the model, in a physically meaningful manner, by adding additional force constants in an empirical manner. We have added second-neighbor central-force couplings, to find no improvement in the fit, as judged by the rms deviation between calculated frequencies and the set of experimental data points.

The simple model fails to fit the elastic constants of copper adequately, of course, since within it the Cauchy relation $c_{12} = c_{44}$ necessarily holds.¹⁴ This relation is violated in copper, as it is in numerous other simple metals. In this paper we are concerned with short-wavelength lattice vibrations almost exclusively, and in our view the lack of a fit to the elastic constants is of no great concern, in view of the overall good account of the phonon spectrum provided by the nearest-neighbor model, throughout the Brillouin zone.

Bortolani and collaborators, in their treatment of Ag and Au,⁵ and their recent study of Cu,⁶ account for the violation of the Cauchy relation by introducing angle-bending terms into the dynamical matrix. These have their origin in three-body interactions, and thus incorporate physics beyond that contained in any pair-potential model. They fit the elastic constants exactly; in the end their model description of the bulk-phonon spectrum contains 23 phenomenologically determined parameters. Their final fit to the bulk-phonon spectrum is excellent.¹⁴

However, it is not clear that in simple metals such as

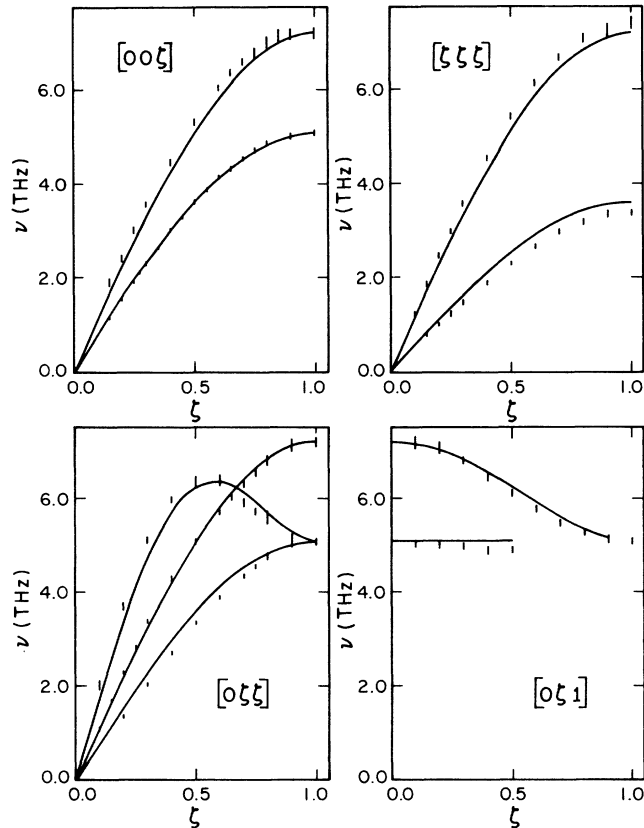


FIG. 1. Comparison between phonon frequencies calculated within the nearest-neighbor central-force model and the neutron data for Cu reported in Ref. 12. The errors in the experimental frequency determination are indicated in the figure. The one parameter in the model, $k_0 = \phi''/M$, assumes the value where ϕ'' is the second derivative of the nearest-neighbor potential and M the atomic mass.

the noble metals the deviation from the Cauchy relation displayed by the elastic constants arises only from angle-bending contributions to the dynamical matrix, whose physical origin is in directional bonding. From *ab initio* theories of the phonon spectra of metals¹⁵ another source is found to be dominant in nearly-free-electron metals. If one expands the total energy in powers of the pseudopotential, the second-order term may be viewed as describing pairwise interactions between nuclei, very similar to those envisioned in phenomenological pair-potential models of lattice dynamics. There is also a zeroth-order term dependent on only the volume of the unit cell, and independent of the atomic arrangement. From the physical point of view, as the crystal expands or contracts, this term has its origin in the work done by the pressure associated with the conduction electrons. If one examines the elastic constants predicted in a model description which contains the zeroth-order term supplemented by those quadratic in the pseudopotential, one finds the Cauchy relation violated.¹⁵ Angle-bending contributions appear first in the terms third order in the pseudopotential, and are thus absent in a calculation which retains only the quadratic terms.

Quite recently, Eguiluz *et al.* have carried out an

ab initio calculation of the bulk-phonon spectrum of aluminum,¹⁶ by retaining the zeroth-order terms, along with those quadratic in the pseudopotential. With no adjustable parameters, a truly excellent fit to the bulk-phonon spectrum is obtained. Also, the elastic constants are given very accurately; in aluminum, the Cauchy relation is violated dramatically. This study establishes clearly that in aluminum angle-bending contributions to the dynamical matrix are very small indeed, and the deviations in the Cauchy relation are due exclusively to the volume-dependent terms in the expression for the total energy. In the noble metals, clearly more directional bonding is present, but at the same time it is unlikely that that deviations from the Cauchy relation have their origin in *only* noncentral contributions to the dynamical matrix, as assumed in the earlier analyses.^{5,6} In the absence of guidance from *ab initio* calculations, we shall confine our attention to the simple nearest-neighbor model which, as we see from Fig. 1, reproduces the bulk-phonon spectrum rather well, throughout much of the Brillouin zone.

We next turn to our description of the surface lattice vibrations on Cu(111). Following the proposal Ref. 5, we suppose the modifications of the intralayer force constant within the surface are of the greatest potential interest. The absence of surface relaxation on Cu(111) also suggests this is reasonable. Thus, we introduce one additional parameter in our description of the surface lattice dynamics, that is, the ratio of the intralayer force constant in the surface relative to that in the bulk.

To see whether this approach is reasonable, we have compared the description of surface lattice dynamics obtained with this approach with that which follows from the work of Jayanthi and co-workers.⁸ We refer to the picture set forth in their work as a semimicroscopic model. The spirit is similar to a shell model, but quadrupole rather than dipole polarizabilities describe the ion cores, to mimic the role of nuclear-displacement-induced virtual *s-d* transitions on the electronic charge distribution. Localized "quasiparticles" of very light mass are introduced to describe the electrons which participate in bonding ions together. These also are endowed with quadrupole polarizabilities. The model provides an excellent description of the bulk-phonon spectrum with only four parameters, each with a clear physical origin. To describe the lattice dynamics of the surface, these authors argue that within the surface layer the ion-core quasiparticle spring constant is altered in a manner that may be inferred quantitatively from data on the static properties of the surface. The calculation produces the longitudinal resonance found in the He-scattering data⁴ as a prominent feature in the spectral density for longitudinal atomic motions in the surface layer (parallel to the surface and parallel to the wave vector transfer Q_{\parallel} experienced by the He atom when the vibration is excited). Jayanthi *et al.* have not calculated the contribution of the longitudinal resonance to the inelastic He-scattering cross section, however.

We compare our model to that developed by Jayanthi *et al.* as follows: we argue that their alteration of the ion-core quasiparticle coupling constant, in the end, leads

to a softening of the effective nearest-neighbor ion-core-ion-core coupling constant. Thus, we inquire if we can choose a value of the intraplanar force constant of our model which reproduces their results. As remarked in Sec. I, the frequency of the high-frequency surface phonon at \bar{M} in the two-dimensional Brillouin zone is quite sensitive to this force constant, since the atom motion within the surface layer is predominantly longitudinal when this mode is excited. Thus, we choose the surface force constant so the gap mode in our model has a frequency identical to that which emerges from the analysis of Jayanthi *et al.*, which is 197 cm^{-1} . We find that a 30% softening of the surface force constant is required for our gap mode to agree with theirs.

A test of the reasonableness of this view is provided in Fig. 2. In Figs. 2(a) and 2(b) we show the spectral density of atomic motions at \bar{M} provided by the model of Ref. 8, for motions normal to the surface (ρ_{zz}) and for longitudinal motions parallel to the surface (ρ_{xx}). We show the spectral densities for motions in the surface layer and in

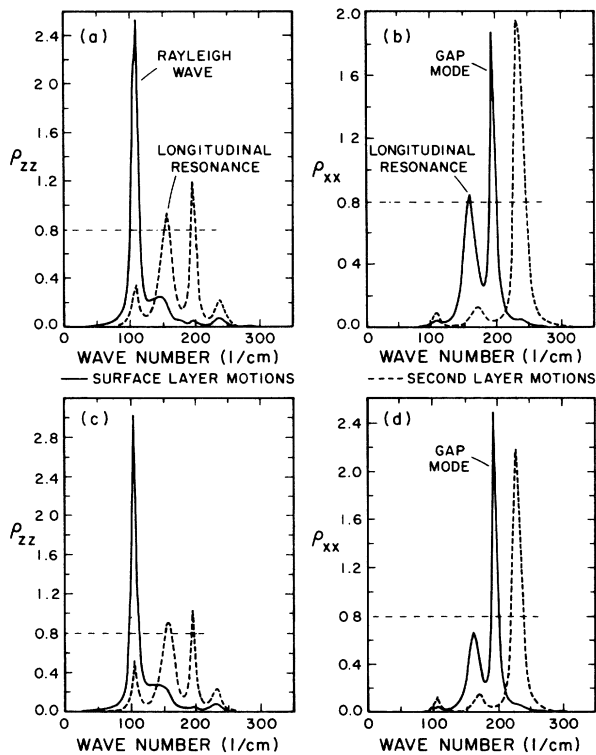


FIG. 2. We give, for the model set forth in Ref. 8, the spectral densities (a) ρ_{zz} for atomic motions in the first and second layers normal to the surface, and (b) ρ_{xx} for atomic motions in the first and second layers parallel to the surface, and to the wave sector \mathbf{Q}_{\parallel} . In both cases \mathbf{Q}_{\parallel} lies at the \bar{M} point of the surface Brillouin zone. The spectral densities are calculated by the prescription used in Ref. 10, and in earlier papers cited therein. In (c) and (d) we give the same spectral densities, generated from the nearest-neighbor central-force model, with bulk force constant chosen as described in Sec. II and with the surface force constant reduced 30% relative to the bulk. Dimensionless units (the same for all four panels) have been employed. The horizontal dashed line is drawn as an aid to the eye.

the second layer. Then, in Figs. 2(c) and 2(d) we show the same spectral densities, calculated with the same scheme, for first- and second-layer motions, with our model and a 30% reduction in intraplanar surface force constant.¹⁷ The agreement between the two sets of spectral densities is excellent, in our view. The principal discrepancy lies in ρ_{xx} (longitudinal motion) in the surface layer, where our model produces a bit more intensity in the gap mode than the model of Ref. 8, and consequently a bit less in the longitudinal resonance. (A sum rule controls the integrated strength of ρ_{xx} , so an excess of strength in the surface model requires less in the longitudinal resonance.) The excess intensity we find in the integrated strength of the gap mode is a bit more than 10%; the integrated strength of this feature is proportional to the square of the eigenvector component which describes parallel motion in the surface layer, so the eigenvector components generated by the two models are in agreement, to the 5% level.

Thus, an appropriate choice of the intraplanar force constant allows our model to mimic quite accurately the description of the surface lattice dynamics of Cu(111) provided by the semimicroscopic model of Ref. 8. Note that the model set forward in Ref. 8 contains a reduction in intraplanar force constant substantially smaller than that invoked in the recent analysis of Cu(111) set forward by Bortolani *et al.*,⁶ and we see the longitudinal resonance appears as a prominent feature in the spectral density which describes atomic motions in the surface layer, parallel to the surface, and to the wave vector \mathbf{Q}_{\parallel} of the vibrational motion. We shall suggest that a 15% rather than a 30% reduction describes the data discussed here very well, for reasons discussed below.

We conclude that the nearest-neighbor central-force model provides a description of the bulk Cu phonons quite adequately for our purpose. If our criterion for a best fit to the bulk-phonon spectrum is employed, it is difficult to see how to improve the model in a physically meaningful manner, without guidance from *ab initio* studies, so far as we can see. We are able also to reproduce very nicely the description of the surface lattice vibrations provided by a rather sophisticated model set forth recently,⁸ by introducing only one more parameter. Thus, we approach the off-specular inelastic-electron-scattering data on Cu(111) using this model, with the surface-layer intraplanar constant as our one free parameter.

III. MULTIPLE-SCATTERING THEORY OF THE EXCITATION CROSS SECTION AND COMPARISON WITH EXPERIMENT

This section is devoted to the discussion of our multiple-scattering calculations for the excitation of surface and bulk phonons on Cu(111) by the incoming electron, and comparison of both the lattice-dynamical model and excitation-cross-section calculations with experiment.

The excitation-cross-section calculations are done within the formalism developed by Li *et al.*,¹¹ which in earlier work has been used with success to calculate the off-specular electron-energy-loss cross sections on several

surfaces, such as Ni(100),^{9,10} Ni(110),³ and also Cu(100).¹⁸ While the theory has been developed in detail elsewhere, we summarize its essential ingredients briefly.

The theory has as its basis a full multiple-scattering description of the electron's interaction with the surface region of the crystal. It enters the crystal and undergoes a sequence of scatterings off the ion cores before it exists. At one of these scatterings it suffers energy loss by creating a surface (or bulk) phonon. Thus, if a multiple-scattering sequence consists of N steps, $N - 1$ events are elastic, and the other is inelastic. We have a sequence of elastic-scattering events on the incoming leg, which is the approach to the site where the inelastic loss occurs, and on an outgoing leg after this event. The total-scattering amplitude is then synthesized by summing over all sites where loss events occur. The sum over all sites within a given layer parallel to the surface is reduced by Bloch's theorem to the loss amplitude at one reference site in the layer, with the constraint that wave-vector components parallel to the surface of all the interacting waves (incident and scattered electron, and the phonon) are conserved, to within a reciprocal-lattice vector. Our past work¹⁰ has established that converged results are obtained if loss sites within the outermost five layers of the crystal are included.

In summing over the possible elastic-scattering sequences, it is natural to break the calculation down into sums over all scatterings within a given layer, and then to link those in various layers together. The basic entities are then a set of layer-diffraction matrices which describe how an electron incident on a given layer (from above or below) which can elastically scatter through or be reflected from the layer. These matrices are amplitudes which connect an incident electron with wave-vector projection $\mathbf{k}_{\parallel} + \mathbf{G}_{\parallel}$ onto a plane parallel to the surface, to final states with wave-vector projection $\mathbf{k}_{\parallel} + \mathbf{G}'_{\parallel}$, where \mathbf{G}_{\parallel} and \mathbf{G}'_{\parallel} are both surface reciprocal-lattice vectors. The layer-diffraction matrices are also functions of the electron's energy E . Hence, for our electron-energy-loss calculation we need two complete sets of such matrices, since the scattered electron wave vector has Fourier components $\mathbf{k}_{\parallel} \pm \mathbf{Q}_{\parallel} + \mathbf{G}_{\parallel}$, with \mathbf{Q}_{\parallel} the wave-vector component of the phonon parallel to the surface involved in the scattering event; one choice of sign describes phonon creation and the other phonon annihilation. We supplement these two sets with a layer matrix that describes intralayer scatterings with the phonon-creation event as one scattering event, and then, by employing methods similar to those developed for the theory of low-energy electron diffraction (LEED),^{19,20} we may synthesize the final-scattering amplitude by stacking the layer matrices.

We have used a modification of the renormalized-forward-scattering (RFS) technique to stack the layers together, and to calculate the LEED intensities of the incident and exiting beam in the inelastic cross section analysis. The RFS method is a perturbation expansion which expands the total-scattering amplitude as a series in the backreflection matrices.²¹ The point is that forward-scattering amplitudes are large but backward-scattering amplitudes are small, in the energy range of interest here. The technique includes all forward scatter-

ings, but only a limited number of backscatterings. It is thus much faster than more exact methods, such as the layer-doubling method, and generally converges well as long as the interlayer spacing exceeds 1 Å.

We generate the phonon eigenvectors that are required for the excitation cross sections by the standard lattice-dynamical slab method. In earlier work, we have found that a 25 layer slab proves quite adequate to describe the resonances produced by the interaction of bulk phonons with the surface, in addition to the surface-phonon loss features. There are 75 eigenmodes for the 25-layer slab; calculation of the cross section for each, a procedure which is required, can be time consuming. We find that the optimum procedure is to arrange the calculation as follows. For scattering from a particular mode s of wave number \mathbf{Q}_{\parallel} , the principal quantity that is calculated may be written¹⁰

$$\delta f = \sum_{l_z} \sum_{\alpha} \left[\frac{\partial f}{\partial R_{\alpha}(l_z)} \right]_0 e_{\alpha}(\mathbf{Q}_{\parallel}s; l_z), \quad (3.1)$$

where $e_{\alpha}(\mathbf{Q}_{\parallel}s; l_z)$ is the α th Cartesian coordinate of the phonon eigenvector in layer l_z , and $[\partial f / \partial R_{\alpha}(l_z)]_0$ is the derivative of the scattering amplitude for scattering from the initial to the final state with respect to displacement of the reference atom in layer l_z . For a given scattering geometry, we first calculate the derivatives $[\partial f / \partial R_{\alpha}(l_z)]_0$ and store them. For the case where the loss event occurs within the first five layers, there are 15 coefficients that must be calculated. Then for each of the 75 modes the sum over l_z is performed very quickly. In our scattering geometry, where only wave vectors along $\bar{\Gamma}-\bar{M}$ in the surface Brillouin zone are probed, the 25 shear horizontal modes are forbidden to scatter, from symmetry considerations. As a diagnostic aid, we calculate the cross section for each of these, and check to see that we indeed find zero.

Once the cross section for each mode s associated with a given wave vector is calculated, we simulate the loss spectrum by superimposing a sequence of Lorentzian lines,

$$I(\omega) = \frac{1}{\pi} \sum_s \frac{I(\mathbf{Q}_{\parallel}, s) \Gamma}{[\omega - \omega(\mathbf{Q}_{\parallel}, s)]^2 + \Gamma^2}, \quad (3.2)$$

where $I(\mathbf{Q}_{\parallel}, s)$ is the scattering intensity for a single bulk or surface phonon. Past work has shown that this procedure provides an excellent quantitative account of the bulk-phonon resonances and structures which appear in the spectrum.

We wish to emphasize that our calculations of the excitation cross section utilize no adjustable parameters, in the description of the electron-solid interaction. The single-site-scattering phase shifts we use, for example, are those used in earlier LEED work.

Since multiple-scattering effects enter importantly in the theoretical description of the phonon-excitation process, it follows the cross sections for exciting various modes exhibit a strong nonmonotonic dependence on impact energy and scattering angle, in a manner reminiscent of LEED or angle-resolved photoemission intensities. The energy dependence is influenced strongly by the po-

larization properties of a given mode; surface phonons with displacement normal to the surface in the outermost layer have cross sections with dramatically different energy variations than modes with displacement parallel to the surface, as past work has shown,⁹ and as we shall see below. Also, as we shall appreciate, atomic motions in the second layer play an important role. One finds, in practice, that changes in beam energy of only 10 eV can lead to dramatic changes in the off-specular loss spectrum. The challenge to the theory is to use this rich store of information to uniquely identify the frequencies of the various surface modes, their polarization, and constraints on surface geometry necessary to account for the observed energy and angle variations.

As just remarked, the calculations must proceed by assuming a surface geometry, and the match to the data is influenced by this choice.⁹ In the particular case of Cu(111), it is established²² that the surface is unreconstructed, and that the spacing between the first and second layer differs from the bulk spacing by less than 0.5%. We have therefore used a completely unrelaxed surface in the calculations presented here.

Our model of surface lattice dynamics is compatible with this choice, since we choose the force constant which couples the first- and second-layer atoms equal to the bulk force constant. We have attempted fits to the data by altering this force constant, to find poor agreement if it is changed. The frequency of the Rayleigh wave at \bar{M} is influenced sensitively by this force constant, and is very insensitive to the intraplanar force constant in the surface. The Rayleigh wave at \bar{M} , and indeed the whole dispersion curve, is fitted very nicely by the nearest-neighbor model with the force constant between the first and second layers unaltered.

Also required for the calculations are several nonstructural parameters. We have used phase shifts from Burdick's copper potential,²³ which have given an excellent account of the off-specular electron-energy-loss cross sections measured on the Cu(001) surface.¹⁸ The other important nonstructural parameter is the complex inner potential. We have taken the real part of the inner potential to be 9 eV, the same as that used in the Cu(001) work. The imaginary part of the inner potential controls how the electron's wave function is attenuated as it travels through the crystal. This parameter mimics the attenuation produced by processes such as particle-hole excitation. In our work we have used an energy-dependent imaginary part for the inner potential. Its magnitude is 2.5 eV at 90 eV incident energy, and it has an $E^{1/3}$ variation.

The influence of the choice of the imaginary part of the inner potential is illustrated in Fig. 3, where we compare the dependence on this parameter of the relative intensity of the S_1 and S_2 surface phonons at \bar{M} . The S_1 mode is the Rayleigh wave, and at \bar{M} the atomic motions in this mode are almost perpendicular to the surface in the outermost layer, and almost parallel to it in the second layer (see Fig. 2). The dominant contribution to the excitation cross section at the energy shown has its origin to coupling to motions in the outermost layer. The S_2 mode at \bar{M} is the high-frequency gap mode at \bar{M} that is a focus

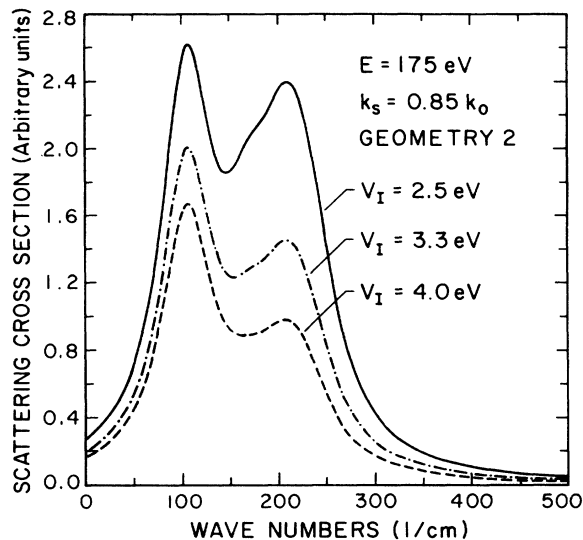


FIG. 3. For a beam energy of 175 eV, and for various choices of the imaginary part of the inner potential V_I , we show calculated loss spectra at \bar{M} . The high-frequency peak is the S_2 -gap surface phonon and the low-frequency peak is the Rayleigh mode. The values quoted for the inner potential are at 90 eV, and we use an $E^{1/3}$ variation of the inner potential, as discussed in the text.

of the present study. For this mode the motions in the outer layer are nearly parallel to the surface and those in the second layer are nearly normal to it (see Fig. 2 again). For S_2 , a large contribution to the cross section comes from coupling to motions in the second layer. Thus, the ratio of the two excitation cross sections is sensitive to the choice of the imaginary part of the inner potential. We see in Fig. 3 that as the imaginary part of the inner potential at 90 eV is changed from 2.5 to 4.0 eV the intensity of S_2 is reduced relative to that in S_1 .

Generally speaking, the cross section for exciting surface modes, or bulk-phonon resonances with atomic displacements parallel to the surface in the outermost layer, is smaller than that for exciting modes with displacement normal to the surface in this layer. From a kinematical point of view one may appreciate why the electron couples to parallel motions in the outer layer less efficiently than perpendicular to it. Such a simple picture shows the cross section to be proportional to $(\Delta\mathbf{k}\cdot\mathbf{u})^2$, with \mathbf{u} the displacement in the mode and $\Delta\mathbf{k}$ the change in wave vector of the electron. For scattering geometries typically used in off-specular electron-energy-loss studies, $\Delta k_{\parallel} \cong \Delta k_{\perp}/10$, so scattering from parallel motions in the outermost layer results in cross sections the order of 1% of those from motions normal to the surface. As remarked in the preceding paragraph, the electron-excitation cross sections also contain contributions from interior layers: it is the case that surface phonons with parallel motions in the outer layer excite perpendicular motions in the second layer, for most high-symmetry points of the surface Brillouin zone, in the low-index surfaces of simple metals. We have just seen that a large contribution to the excitation cross section of the S_2 sur-

face phonon on Cu(111) comes from such second-layer motions, but since the electron's wave function is attenuated appreciably by the time it arrives at the second layer, the excitation cross section of a mode with parallel motions in the surface tends to be substantially smaller than that with motions perpendicular to the surface.

However, earlier theoretical studies of excitation cross sections for surface phonons on the Ni(100) surface have shown that within selected energy ranges often rather narrow multiple-scattering resonances can enhance the cross sections for parallel modes to the point where they become comparable to, or even somewhat larger than, those for perpendicular modes.^{9,24,25} Indeed, the theory predicted selected "energy windows" within which the parallel S_6 surface phonon at the \bar{X} point on Ni(100) can have a cross section comparable to that of the perpendicular S_4 (Rayleigh) mode. Experiments later found these windows, where predicted.⁶

On Cu(111) our calculations also show that selected "windows" exist, within which modes with parallel motions in the surface scatter efficiently. We show this in Fig. 4, where we compare the energy variation of the

cross section for exciting the S_1 (Rayleigh) phonon at \bar{M} and the high-frequency S_2 phonon in the gap of the projected phonon density of states. For beam energies at 110 eV, as through most of the energy ranges scanned in the experimental studies of Cu(111), the Rayleigh mode provides the dominant feature in the loss spectrum. With increasing energy, we find that the Rayleigh cross section decreases, to pass through a sharp deep minimum at 155 eV. This dip in the Rayleigh-wave cross section is found in the experiments, very much as given by theory. However, the S_2 mode is not found in this energy range, because the longitudinal resonance dominates the loss cross section, within the dip. This experimental observation is reproduced nicely by the calculations presented below. In Fig. 4(b) we see that the gap-mode excitation cross section has a maximum near 175 eV; here the cross section of S_2 becomes comparable to that of the Rayleigh modes, and the theory shows the contribution from the longitudinal resonance to the loss cross section is small. It is the case that the experiments resolve the gap mode when the impact energy is 175 eV.

Before we turn to a discussion of the comparison between experiment and theory, we address some experimental considerations. The high-resolution electron-energy-loss (HREELS) measurements were performed with a 127° cylindrical deflection spectrometer consisting of a double-pass monochromator and a single-pass analyzer.²⁴ The energy resolution of the instrument was set to approximately 40–50 cm^{-1} over a primary energy range of 1–240 eV. The Cu(111) surface was oriented along a $(\bar{1}\bar{1}2)$ azimuth by the Laue-reflection method and it was cleaned by cycles of Ar^+ -ion bombardment and annealing to 400°C. Auger analysis showed only trace amounts of carbon impurity, which, however, did not produce any structure in the HREELS spectrum that could be attributed to carbon impurity. Also, the LEED pattern was of excellent quality. All of the phonon measurements were carried out at room temperature.

As has been shown previously,⁹ the inelastic-electron-scattering cross section for phonon modes depends markedly on the primary energy E_0 . Therefore, before the dispersion curve of any phonon mode can be obtained, one needs to search for primary energies that maximize the cross section of that mode. In our case this was done by selecting a value for the momentum transfer, Q_{\parallel} , and measuring the HREELS spectra corresponding to this phonon wave vector at various primary energies until an optimum intensity was found for that mode. Following this procedure, the optimum values for the inelastic-scattering cross section for the Rayleigh (S_1), longitudinal-resonance (LR), and gap (S_2) modes were found at $E_0=110, 150,$ and 175 eV, respectively. After applying a standard smoothing routine, the peak positions of the HREELS spectra were obtained by using a curve-fitting program that was based on Gaussians and which required that the ratio of the intensities of the loss and gain peaks be equal to the Boltzmann factor. Because of the above-mentioned sharp dependence of the phonon cross section on E_0 , only a few apparent modes were present in any given spectrum at the optimum primary energy. Consequently, only a few Gaussians were

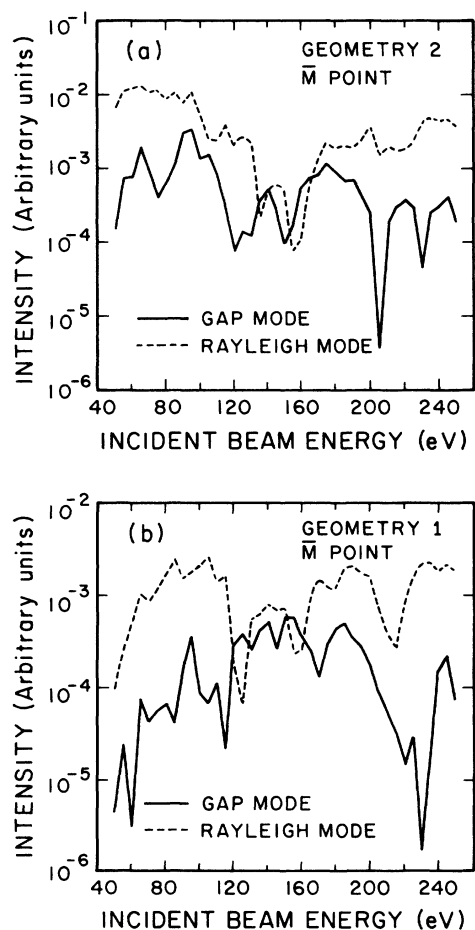


FIG. 4. Energy variation of the gap-mode and Rayleigh-wave cross sections, for these modes at the \bar{M} point of the Brillouin zone, for the two geometries used in the experiments. In geometry 2 the angle of incidences less than the angle of the exciting electron, and the converse is true for geometry 1.

needed to achieve a good fit. For example, at $E_0 = 175$ eV the HREELS spectrum at \bar{M} consists of three features that can be fitted with three Gaussians: one for the peak that corresponds to the diffuse elastic scattering of the impinging electrons, one for the Rayleigh mode, and another for the gap mode. At $E_0 = 110$ eV, however, the spectrum at \bar{M} consists of two features only: the elastic and the Rayleigh peaks, and these can be fitted with two Gaussians. The reliability of the fitting was indicated by the excellent agreement of the peak energies obtained for the Rayleigh mode by fitting to the data of $E_0 = 110$ and 175 eV.

The position on the energy scale of the elastic peak as well as its full width at half maximum (FWHM) is found by first taking a specular spectrum. The FWHM of the Gaussians were made consistent with the FWHM of the elastic peak. Also, a small background correction, typically less than 15% of the peak heights, was made, and the reproducibility of the peak positions was approximately 5 cm^{-1} . In Fig. 5 we show the experimental data points, in the form of dispersion curves, along with a comparison with the theoretical model, as discussed below. For each mode a series of measurements were made at each selected Q_{\parallel} . Therefore, the experimental points shown in the dispersion curves displayed in Fig. 5

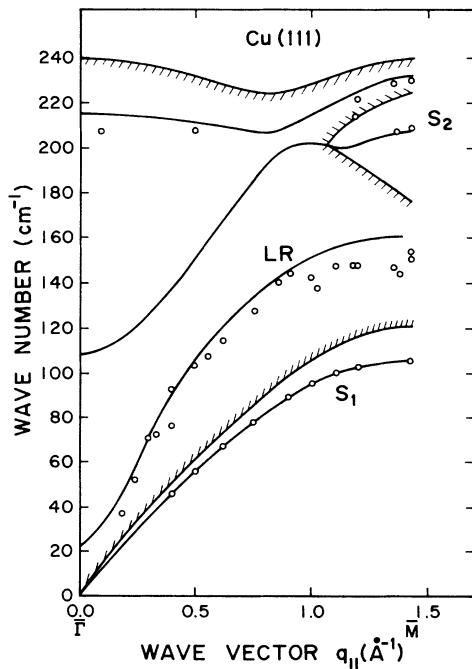


FIG. 5. Experimental data showing the dispersion relation of the Rayleigh wave (S_1), that of the longitudinal resonance (LR), and the frequency of the gap mode (S_2). Other points are placed where structure in the loss spectra has been observed. The data are compared with the predictions of the nearest-neighbor central-force model discussed in the text, for which a 15% softening of the intraplanar force constant within the surface layer is assumed. The hatched area denotes the projection of the bulk-phonon spectrum on the $\bar{\Gamma}-\bar{M}$ line. We also show trajectories of maxima in the calculated cross sections, within the bulk-phonon hands.

represent an average of the peak values obtained from the fitting program. In Fig. 5, in addition to the experimental data, we show the projected bulk-phonon bands as generated by our model (shaded area), along with the dispersion relation of the S_2 gap phonon, the longitudinal resonance, and the Rayleigh wave all shown as solid lines. The theoretical results are generated with the surface intraplanar force constant k_s chosen equal to $0.85k_0$, with k_0 the bulk force constant.

As remarked earlier, where the data reported here overlap with the earlier inelastic-He-scattering data reported by Toennis *et al.*, the two data sets are in very good agreement. The helium data on Cu(111) for both the Rayleigh wave and the longitudinal resonance extend only roughly two-thirds of the way from $\bar{\Gamma}$ to \bar{M} , and the S_2 gap mode was not seen in this work, as remarked in Sec. I.

There is one additional aspect of the present experimental geometry that is interesting, for the (111) surface of a fcc crystal such as copper. In the spectrometer the angle between the monochromator and the detector is fixed at 124° . For specular scattering the angle of incidence can thus be only 62° . To measure energy-loss spectra with $Q_{\parallel} \neq 0$, the crystal is rocked by a manipulator about an axis normal to the scattering plane. The amount the crystal needs to be rocked to access a particular value of $|Q_{\parallel}|$ depend on the electron energy. The rocking angle ϕ_R is determined by the condition

$$\sin(\phi_R) = \frac{Q_{\parallel}}{2k_0 \cos(62^\circ)}, \quad (3.3)$$

where $k_0 = (2mE/\hbar^2)^{1/2}$ is the electron's wave vector.

Thus, with the above apparatus there are two ways of accessing a given value of $|Q_{\parallel}|$. Geometry 1 occurs when $\theta_I > \theta_F$, and has $\phi_R > 0$. Geometry 2 has $\theta_I < \theta_F$ and $\phi_R < 0$. The sign of Q_{\parallel} for geometry 2 is opposite that for geometry 1. If $\omega_j(Q_{\parallel})$ is the frequency of a given bulk or surface phonon of wave vector Q_{\parallel} , one may invoke time-reversal symmetry to prove that $\omega_j(+Q_{\parallel}) = \omega_j(-Q_{\parallel})$. A measurement at $+\phi_R$ and $-\phi_R$ thus probes modes of the same frequency.

However, if we consider a given frequency, it is a peculiar feature of the (111) surface that the excitation cross sections at $+Q_{\parallel}$ and at $-Q_{\parallel}$, in general, differ, with Q_{\parallel} directed along the $\bar{\Gamma}-\bar{M}$ line. The surface layer, considered in isolation from the rest of the crystal, has a six-fold axis. For scattering from such an isolated layer the existence of a reflection plane normal to the scattering plane allows one to prove that the excitation cross sections at $+Q_{\parallel}$ and $-Q_{\parallel}$ are identical. However, by virtue of the position of the second layer relative to the first, in the semi-infinite Cu(111) structure the symmetry axis of the semi-infinite crystal is a threefold axis, the reflection plane is then lacking, and, in principle, the two cross sections differ. The wave functions of both the incoming and scattered electrons sense the lack of a reflection plane, and also the phonon eigenvector at $+Q_{\parallel}$ differs from that at $-Q_{\parallel}$.

Figure 4 shows an example of this difference, as a function of energy, at the \bar{M} point. Experimentally, it was

found that the intensity of the Rayleigh mode for geometry 2 is a factor of 3 higher than for geometry 1, at $E = 110$ eV. Our theory predicts the ratio to be 2.3, quite close to this result. We can reproduce in a systematic way the differences found for the two geometries; the electron-energy-loss cross-section data can then be used as a means of deciding which of the two possible inequivalent orientations is realized, when the crystal is in the spectrometer.

The sensitivity of the cross sections to orientation of the (111) surface just discussed may prove useful in other contexts. For instances, adsorbates will tend to chemisorb in the threefold hollow sites. On the (111) surface of a fcc crystal there are two distinctly different hollow sites. One of these, referred to as the hcp site, has a second-layer atom directly below the hollow. The second is the fcc site, for which there is no second-layer atom underneath. It is of considerable interest to know which of these two sites is preferred for chemisorption.²⁶ In Fig. 6 we illustrate the two scattering orientations, geometry 1 and geometry 2, used to probe the $\bar{\Gamma}-\bar{M}$ line of the clean surface in the present study. In Fig. 6(a) the hcp site is on the negative y axis and the fcc site is on the positive axis. This illustrates scattering along the $[11\bar{2}]$ direction. The situation is reversed in Fig. 6(b), which is scattering along $[\bar{1}\bar{1}2]$. As we have seen, the various scattering cross sections along these two directions show distinctly different energy variations. If the surface has a chemisorbed overlayer, it follows that the energy variation of the cross sections for exciting modes in the overlayer will also differ substantially for an overlayer in the hcp site and one in the fcc site. With data for an adsorbate-covered surface such as that discussed here for the clean surface, in combination with theoretical calculations, one should be able to discriminate between the two adsorption sites.

There is a relation between the scattering cross sections

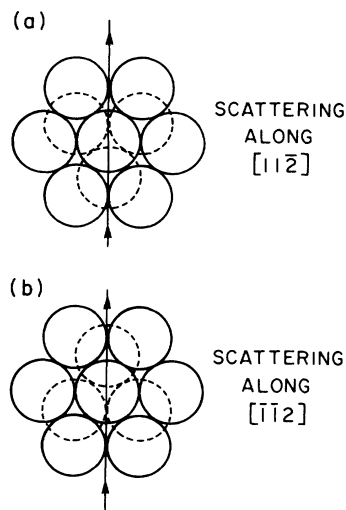


FIG. 6. Schematic drawing of the two incident-beam directions discussed in the text: (a) the $[11\bar{2}]$ direction and (b) the $[\bar{1}\bar{1}2]$ direction. We are looking down on the surface; the solid circles are atoms in the outermost layer and the dotted lines are atoms in the second-layer atoms, for various scattering geometries discussed in the text.

for geometries 1 and 2, and it is the following. The cross section for geometry 1, with the beam incident along $[11\bar{2}]$, is the same as for geometry 2, with the beam along $[\bar{1}\bar{1}2]$, and conversely. One may see this with the aid of Fig. 7. Figure 7(a) shows the incident- and scattered-electron directions for geometries 2 and 1, for the electron incident along $[11\bar{2}]$. Now consider what happens if we time-reverse the scattering process for geometry 2, as shown in Fig. 7(c). Because of microreversibility, the matrix element for the time-reversed process (in which a phonon is annihilated) is the same as that for the original process (in which a phonon is created). Now if we suppose that the electron's wave function changes little when the electron energy is shifted by the phonon energy (an assumption violated in the near vicinity of fine-structure resonances, as shown explicitly in earlier calculations²⁷), then it follows that to very high accuracy the matrix element for phonon creation and annihilation in Fig. 7(c) is the same. We conclude that the phonon-excitation cross section is the same for geometry 1 with the electron incident from the right, as in Fig. 7(c), as that for geometry 2 with the electron incident from the left, as in Fig. 7(a). In Fig. 7(d), Fig. 7(c) has been rotated by 180° , so the in-

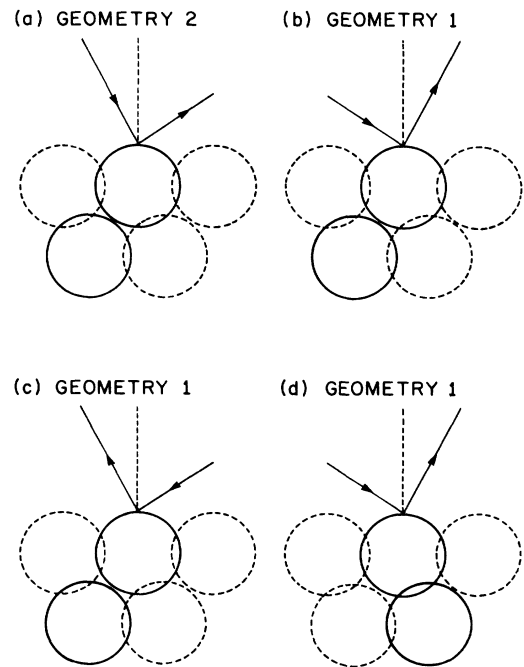


FIG. 7. Here we show a side view of the various scattering geometries. In each panel the atoms depicted as solid circles lie in the plane normal to the surface, which also contains the incident beam depicted in Fig. 6. The dashed circles depict the first- and second-layer sites which lie in the adjacent plane, parallel to that just described, which contains the next vertical column of nuclei. The panels then illustrate (a) geometry 2, incident beam along $[11\bar{2}]$; (b) geometry 1, beam incident along $[11\bar{2}]$; (c) geometry 1, beam incident along $[11\bar{2}]$, but the crystal is rotated 180° with respect to the orientation in $[11\bar{2}]$.

cident and scattered directions are the same as in Fig. 7(b), which is the geometry also illustrated in Fig. 6(b), while Fig. 7(d) then becomes equivalent to Fig. 6(a).

We encountered the above relationship in the following manner. The initial theoretical loss cross-section calculations provided a rather poor account of the data. As more data became available, it became apparent that we obtain an excellent account of the data by interchanging the results of geometries 1 and 2. The model crystal in the theorists' computer was rotated with respect to that in the spectrometer by 180° , and this accounted for the problem. The off-specular energy-loss cross-section calculations can then indeed be used to determine which of the two inequivalent orientations are realized in the spectrometer. As remarked above, it would be of considerable interest to perform calculations on a (111) surface with an ordered overlayer present, to determine which of the two inequivalent hollow sites are occupied by the adsorbates, as discussed above.

In Fig. 8 we show a comparison between experiment (the solid line) and theory at the \bar{M} point, for three different energies and geometry 2. There are three theoretical curves, corresponding to three choices of intraplanar surface force constant. The dashed line is for $k_s = 0.85k_0$, the dotted line is for $k_s = 0.70k_0$, and the dotted-dashed line is $k_s = 0.50k_0$, with k_s and k_0 the surface and bulk force constants. In Fig. 8(a), for a beam energy of 110 eV, the spectrum is dominated by the Rayleigh wave at 107 cm^{-1} . The slight asymmetry on the high-frequency side of the main peak is a contribution from the longitudinal resonance, which is quite weak at this beam energy. Also, there is a shoulder in the vicinity of 225 cm^{-1} that has its origin in bulk phonons which have frequency above the gap in the projected bulk-phonon density of states at \bar{M} . The various vertical lines shown at the bottom of the panel show the intensities of the strongest surface- and bulk-phonon modes which emerge from our slab calculation. We clearly see the packet of modes from which the longitudinal resonance is formed.

Figure 8(b) compares theory and experiment for a beam energy of 150 eV. There are two principal contributions to the spectrum. The major peak at 152 cm^{-1} is the longitudinal resonance. The peak at 228 cm^{-1} is the result of a concentration of bulk modes above the gap at \bar{M} which contribute strongly to the spectral density for longitudinal motions in the second layer.

Finally, in Fig. 8(c) we clearly see the gap mode S_2 . For 175 eV the S_2 and Rayleigh modes dominate the spectrum, with the gap mode clearly resolved. The high-frequency bulk modes, whose influence is evident in Figs. 8(a) and 8(b), contribute virtually nothing to the loss spectrum at this energy.

We next turn to the question of the amount of softening we require for the intraplanar force constant in the surface layer. If we fit the frequency measured for the S_2 -gap phonon at \bar{M} , we require a 15% softening of the force constant, as discussed earlier. We see in Fig. 8 that this choice also results in good fits to both systematics of the excitation cross sections, though we then find that the frequency of the longitudinal resonance at \bar{M} is slightly

higher than measured. Note that with the modest softening just described, we have no difficulty reproducing the intensity of the longitudinal resonance, as seen in the data. In Fig. 9 we show the variation of the frequency of

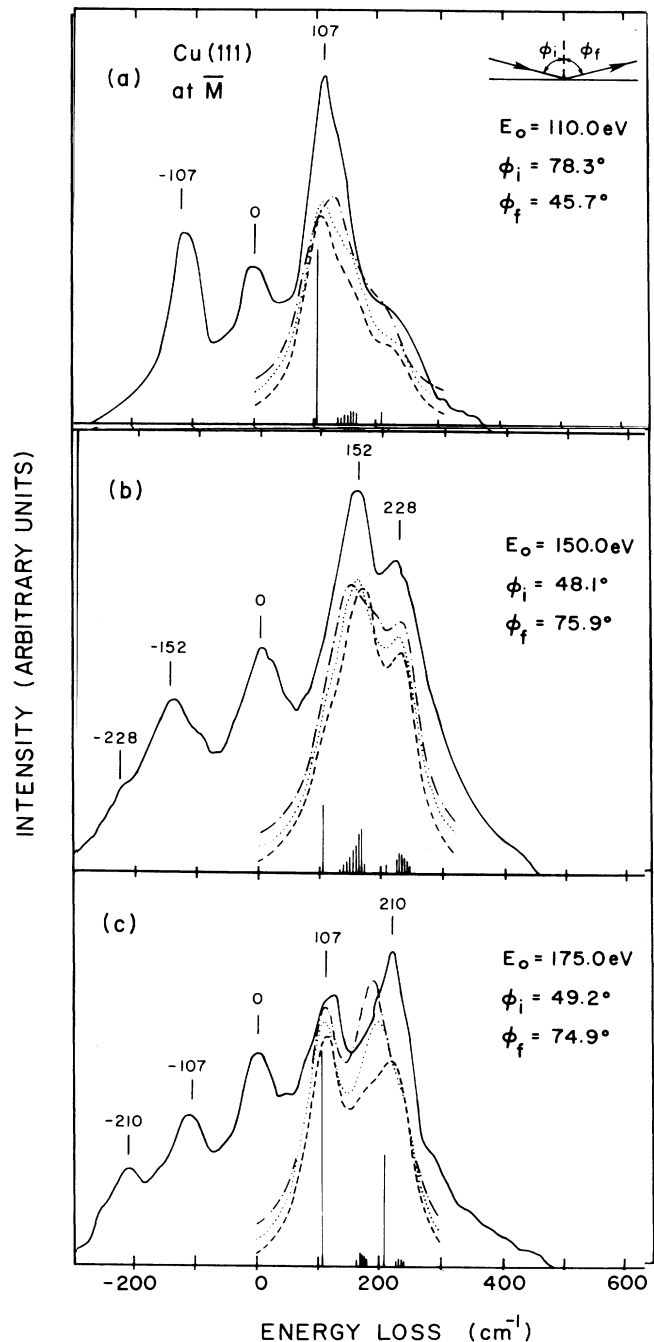


FIG. 8. Experimentally measured loss cross sections at energies of (a) 110.0 eV, (b) 150.0 eV, and (c) 175.0 eV and at the scattering angles indicated. We compare the data with calculations based on three lattice-dynamical models: (i) intraplanar surface force constant softened 15% (dashed line), (ii) intraplanar force constant softened 30% (dotted line), and (iii) intraplanar force constant softened 50% (dashed-dotted line). We also show the intensities of individual bulk- and surface-phonon modes of our 25-layer slab. We illustrate only those modes which scatter with non-negligible intensity.

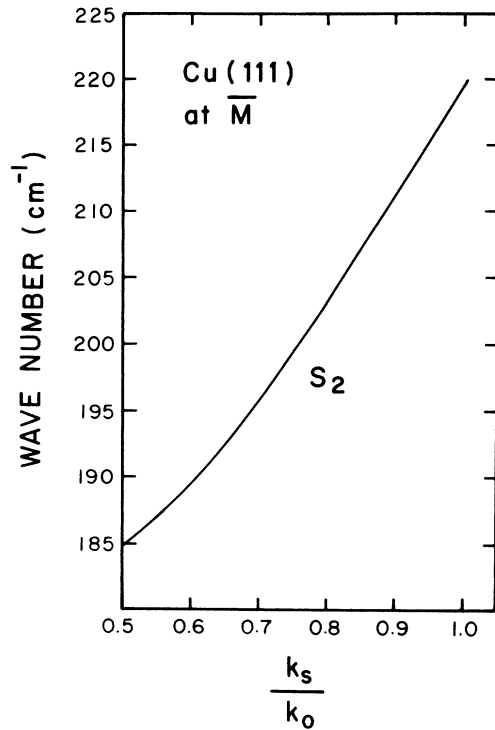


FIG. 9. Within our nearest-neighbor central-force model, we show the frequency of the S_2 -gap phonon, as a function of the ratio k_s/k_0 , where k_0 and k_s are the bulk force constants, and that within the surface layer.

the gap mode with surface force constant k_s . As remarked earlier, the choice $k_s=0.7k_0$ reproduces the frequency, 197 cm^{-1} , that emerges from the theory of surface lattice dynamics set forth by Jayanthi *et al.* However, this lies well below the experimental value.

In Fig. 10 we compare the data with theoretical loss spectra for points along the line from $\bar{\Gamma}$ to \bar{M} , for $k_s=0.85k_0$.

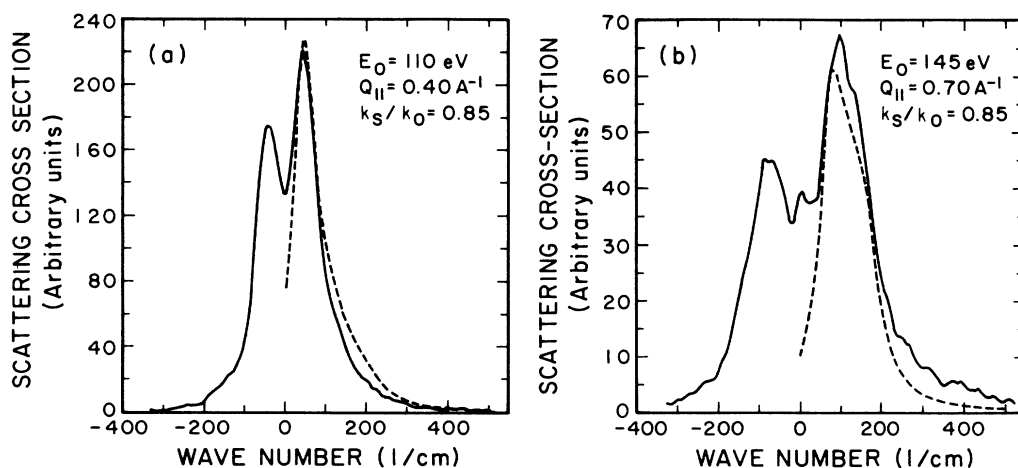


FIG. 10. Comparison between the theoretical loss spectrum (dashed line) and data (solid line), for two values of Q_{\parallel} on the line between $\bar{\Gamma}$ and \bar{M} . We compare the theory and experiment only on the energy-loss side of the line. The comparisons are for (a) $E_0=110\text{ eV}$ and $Q_{\parallel}=0.40\text{ \AA}^{-1}$ and (b) $E_0=145\text{ eV}$ and $Q_{\parallel}=0.70\text{ \AA}^{-1}$.

In our view, the present analysis rules out very large changes in intraplanar force constant, such as the 70% softening proposed by Bortolani and collaborators. Such a large softening not only produces a frequency for the S_2 mode that is far too low, but if we use such large softening we are also unable to reproduce the loss cross sections with our theory. This is evident in Fig. 8, where we also show a comparison between theory and experiment for the case where $k_s=0.5k_0$.

One might inquire if our rather simple model of surface lattice dynamics, with a very large softening of surface force constants, produces a picture of the surface spectral densities similar to that from the very sophisticated model developed by Bortolani *et al.* They find 177 cm^{-1} for the S_2 mode at \bar{M} , and if we set $k_s=0.3k_0$ as they suggest, we find a frequency very close to this value, as is evident from a simple extrapolation of the curve in Fig. 9. Thus, while we have not made a detailed comparison between the predictions of our model, with $k_s=0.3k_0$ and theirs, we expect that by choosing $k_s=0.3k_0$ we will obtain a description of the surface lattice dynamics rather similar to theirs.

In Sec. II we compared the spectral densities generated by our lattice-dynamical model using $k_s=0.7k_0$ with those generated by the model of Jayanthi *et al.* The comparison is given in Fig. 2. We have also used their eigenvectors to calculate the off-specular electron-energy-loss cross sections, and compare the results with cross sections produced from our model with the choice $k_s=0.7k_0$. For three electron energies, we present the results in Fig. 11. The dotted lines are results obtained with the nearest-neighbor model and the choice $k_s=0.7k_0$, and the solid lines are generated from the lattice-dynamical model in Ref. 8. The two sets of results are almost identical, which suggests that the description of the short-wavelength response of the surface region is rather insensitive to fine details of lattice-dynamical models which provide common values for the frequencies of

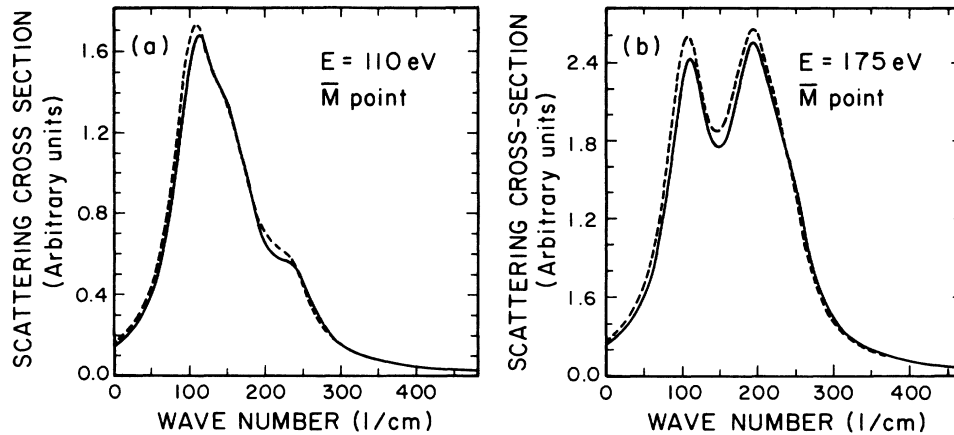


FIG. 11. Comparison between the energy-loss spectra at \bar{M} , calculated with our nearest-neighbor model and a 30% reduction in intraplanar force constant (dashed line), and the loss spectrum generated using the eigenvectors generated by the model of Jayanthi, Bilz, Kress, and Benedek (Ref. 8). We compare at two energies: (a) 110 eV and (b) 175 eV.

motion of various characteristic frequencies.

If one sets the conclusions of the present study alongside our earlier analyses of the surface lattice dynamics of low-index unreconstructed faces of simple metals, one concludes that all such surfaces are described rather quantitatively by simple models of the surface region, within which the force constants assume values within 10% or 20% of their bulk values. Even for Ni(110), where there is a large contraction between the first and second layers, the relaxation produces roughly a 30% stiffening of the force constant which couples atoms in first and third layers. It will be of great interest to set

these conclusions alongside those which emerge from future *ab initio* calculations.

ACKNOWLEDGMENTS

We wish to thank A. Ormeci for his assistance with the numerical calculations, and M. Hosek for technical assistance. Two of us, B.M.H. and D.L.M., were supported by the U.S. Department of Energy (DOE) through Grant No. DE-FG03-84-ER45083, and two others M.H.M. and L.L.K. by the DOE through Grant No. DE-FG02-84-ER45147.

¹G. Brusdeylins, R. B. Doak, and J. P. Toennies, Phys. Rev. Lett. **46**, 437 (1981); Phys. Rev. B **27**, 3662 (1983).

²S. Lehwald, J. Szeftel, H. Ibach, Talat S. Rahman, and D. L. Mills, Phys. Rev. Lett. **50**, 518 (1983).

³S. Lehwald, F. Wolf, H. Ibach, Burl M. Hall, and D. L. Mills, Surf. Sci. **192**, 131 (1987).

⁴U. Harten, C. Wöll and J. P. Toennies, Phys. Rev. Lett. **55**, 2308 (1985); U. Harten, J. P. Toennies, and C. Wöll, Faraday Disc. Chem. Soc. **80**, 137 (1985).

⁵V. Bortolani, A. Franchini, F. Nizzoli, and G. Santoro, Phys. Rev. Lett. **52**, 429 (1984). Also see the discussion by V. Bortolani and G. Santoro, in *Phonon Physics* (Proceedings of the Second International Conference on Phonon Physics), edited by J. Kollar, N. Kroo, N. Menyhard, and T. Siklos (World Scientific, Singapore, 1985), p. 566.

⁶G. Santoro and V. Bortolani (private communication).

⁷R. E. Allen, G. P. Alldredge, and F. W. de Wette, Phys. Rev. B **4**, 1661 (1971).

⁸C. S. Jaynathi, H. Bilz, W. Kress, and G. Benedek, Phys. Rev. Lett. **59**, 795 (1987).

⁹M. L. Xu, B. M. Hall, S. Y. Tong, M. Rocca, H. Ibach, S. Lehwald, and J. E. Black, Phys. Rev. Lett. **54**, 1171 (1986).

¹⁰Burl M. Hall and D. L. Mills, Phys. Rev. B **34**, 8318 (1986).

¹¹S. Y. Tong, C. H. Li, and D. L. Mills, Phys. Rev. Lett. **44**, 407 (1980); C. H. Li, S. Y. Tong, and D. L. Mills, Phys. Rev. B **24**, 806 (1981).

¹²Mohamed H. Mohamed, L. L. Kesmodel, Burl M. Hall, and

D. L. Mills, Phys. Rev. B **37**, 2763 (1988).

¹³E. C. Svensson, B. N. Brockhouse, and J. M. Rowe, Phys. Rev. **155**, 619 (1967).

¹⁴See the discussion which begins on p. 95 of C. Kittel, *Introduction to Solid State Physics*, 2nd ed. (Wiley, New York, 1953).

¹⁵See the discussion that has been presented by E. G. Brovman and Y. Kagan, in *Dynamical Properties of Solids*, edited by A. A. Maradudin and G. Horton (North-Holland, Amsterdam, 1974), Vol. 1, p. 191.

¹⁶See Fig. 1 of A. G. Eguiluz, A. A. Maradudin, and R. F. Wallis, Phys. Rev. Lett. **60**, 309 (1988).

¹⁷We wish to express our gratitude to Dr. C. S. Jayanthi for providing us with the eigenvectors and eigenfrequencies at \bar{M} generated by the model of Ref. 8. This enabled us to compare the two sets of spectral densities quite directly, each generated by our subroutines and conventions.

¹⁸L. L. Kesmodel, M. L. Xu, and S. Y. Tong, Phys. Rev. B **34**, 2010 (1986).

¹⁹S. Y. Tong, Prog. Surf. Sci. **7**, 1 (1975).

²⁰The renormalized forward-scattering method is discussed in J. Pendry, *Low Energy Electron Diffraction: The Theory and Its Application to the Determination of Structures* (Academic, London, 1974).

²¹Burl M. Hall, Ph.D. thesis, University of Wisconsin-Milwaukee, 1983.

²²H. L. Davis and J. R. Noonan, Surf. Sci. **176**, 245 (1983).

²³G. A. Burdick, *Phys. Rev.* **125**, 138 (1963).

²⁴L. L. Kesmodel, *J. Vac. Sci. Technol. A* **1**, 1456 (1983).

²⁵For a detailed discussion of the contributions of parallel and perpendicular motions in various layers to the off-specular excitation cross sections on Ni(100), see D. L. Mills and S. Y. Tong, *Philos. Trans. R. Soc. London, Ser. A* **318**, 179 (1986).

²⁶For an example where this question has arisen, we refer the reader to Talat S. Rahman, J. E. Black, and D. L. Mills, *Phys. Rev. B* **27**, 4059 (1983).

²⁷Burl M. Hall, S. Y. Tong, and D. L. Mills, *Phys. Rev. Lett.* **50**, 1277 (1983).